ChemComm

COMMUNICATION

View Article Online
View Journal | View Issue

Cite this: *Chem. Commun.*, 2014, **50**, 7117

Received 21st March 2014,
Accepted 15th May 2014

DOI: 10.1039/c4cc02123a

www.rsc.org/chemcomm

$LiFePO_4$ nanoparticles encapsulated in graphene nanoshells for high-performance lithium-ion battery cathodes†

Huilong Fei,[a] Zhiwei Peng,[a] Yang Yang,[b] Lei Li,[a] Abdul-Rahman O. Raji,[a] Errol L. G. Samuel[a] and James M. Tour*[abc]

$LiFePO_4$ encapsulated in graphene nanoshells ($LiFePO_4$@GNS) nanoparticles were synthesized by solid state reaction between graphene-coated Fe nanoparticles and LiH_2PO_4. The resulting nanocomposite was demonstrated to be a superior lithium-ion battery cathode with improved cycle and rate performances.

Lithium iron phosphate, $LiFePO_4$, is considered to be the most promising cathode material due to its low cost, low toxicity, and high safety.[1,2] However, its lithium storage performances are limited by its poor rate capability (fast decay of specific capacity at high charge–discharge rate) resulting from the intrinsically slow diffusion of Li^+ through its one dimensional structural channels and low electrical conductivity.[3,4] Numerous efforts have been tried to address this problem by tailoring the particle size into the nano-range to decrease the ionic and electrical path length and/or by conductive coating (carbon coating in particular) to enhance the electrical conductivity.[5,6]

Traditionally, $LiFePO_4$ is synthesized by solid state reaction at high temperature (typically >600 °C), at which nanoparticles tend to melt or aggregate to form larger particles.[7] To circumvent this problem and achieve nano-sized $LiFePO_4$, some low-temperature methods have been developed but with the sacrifice of crystallinity, and thus the resulting $LiFePO_4$ suffered from low electrochemical stability.[1,8] As a result, solid state reaction still remains the most effective method to obtain highly crystalline $LiFePO_4$ with olivine structure.

As for carbon-coated $LiFePO_4$, various synthetic coating methods and the effect of carbon coating quality on the properties of the C–$LiFePO_4$ composite have been recently reviewed and it was emphasized that uniform and highly graphitic carbon coatings are ideal, which ensures efficient electron transfer between $LiFePO_4$ particles.[9] Up to now, most of the carbon coating strategies involve the addition of carbon-containing precursors (such as citric acid, glucose, and benzene) into lithium, iron and phosphorus sources during the formation of $LiFePO_4$ by solid state reaction, hydrothermal reaction and sol–gel reaction.[10–12] However, the as-obtained carbon coatings were not uniform and the coated carbon was mainly amorphous with limited improvement of conductivity. The highly conductive graphitic carbon could only be obtained in the presence of metallic catalyst (*e.g.* Fe, Co and Ni) at relatively low temperature.[11]

The above background suggests that it remains a challenge to achieve a uniform and high quality (graphitic) carbon coating while producing the $LiFePO_4$ particle in the nanosize range.[2,5,9] In this communication, we have obtained highly crystalline $LiFePO_4$ nanoparticles encapsulated in graphene nanoshells ($LiFePO_4$@GNS) by performing solid state reactions between metallic Fe^0 encapsulated in graphene nanoshells (Fe@GNS) and LiH_2PO_4. Benefiting from the highly conductive graphene shells and nano-sized $LiFePO_4$, the $LiFePO_4$@GNS nanocomposite exhibits excellent cycle and rate performances when used as a cathode material for lithium-ion batteries.

The starting material Fe@GNS was prepared according to our recently reported CVD coating method by using CH_4 as carbon source and graphene oxide sheets as space restrictors to prevent high temperature aggregation (see ESI† for Experimental details).[13] As shown in Fig. 1a and b, this nanocomposite consists of Fe@GNS nanoparticles with a core–shell structure by transmission electron microscopy (TEM). The as-formed carbon coating is uniform, continuous and graphitic due to the use of the metallic Fe^0 catalyst for carbon growth. As illustrated in Fig. 1c, to transform Fe@GNS into $LiFePO_4$@GNS, Fe@GNS was first mixed with LiH_2PO_4 and heated in air at 300 °C for 8 h to oxidize Fe^0 to Fe^{3+}. The mixture was then annealed at 500 °C for 8 h in a slightly reducing atmosphere ($Ar:H_2 = 95\%:5\%$) to allow the reaction between the carbon-coated interior Fe source with the exterior Li and P sources to form $LiFePO_4$. During this solid state reaction process, severe

[a] *Department of Chemistry, Rice University, 6100 Main Street, Houston, Texas 77005, USA. E-mail: tour@rice.edu*
[b] *The Smalley Institute for Nanoscale Science and Technology, Rice University, 6100 Main Street, Houston, Texas 77005, USA*
[c] *Department of Materials Science and NanoEngineering, Rice University, 6100 Main Street, Houston, Texas 77005, USA*

† Electronic supplementary information (ESI) available: Experimental and characterization details, additional XPS, SEM, TGA data. See DOI: 10.1039/c4cc02123a

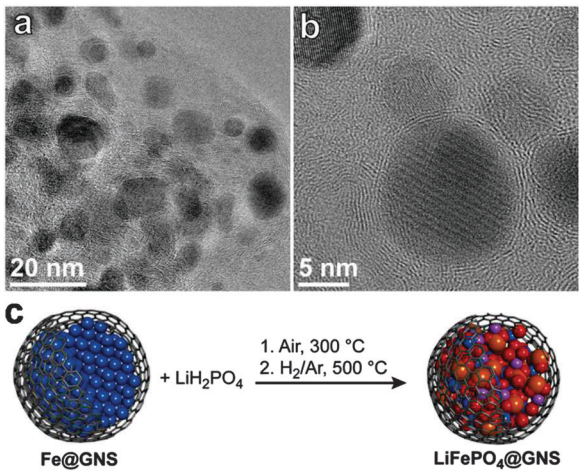

Fig. 1 TEM images of Fe@GNS with core–shell structures at (a) low and (b) high magnifications. (c) Scheme illustrating the synthetic route to $LiFePO_4$@GNS, starting from Fe@GNS.

high temperature aggregation of the nanoparticles was avoided with the presence of graphene layers, which acted as protective shells due to their high thermal and chemical stability. By this synthetic design, nanosized $LiFePO_4$ was obtained with a uniform graphitic carbon coating.

Fig. S1 (ESI†) shows the X-ray photoelectron spectroscopy (XPS) survey spectra of Fe@GNS and $LiFePO_4$@GNS, which indicates the absence of contaminants. Fig. 2a compares the Fe $2p_{3/2}$ spectra of $LiFePO_4$@GNS and Fe@GNS. The Fe in the Fe@GNS was in metallic form (~707 eV); however, after the solid state reaction, the Fe in $LiFePO_4$@GNS was in Fe^{2+} form (~711 eV),[14] consistent with the Fe oxidation state in $LiFePO_4$. X-ray diffraction (XRD) was then used to identify the phase of as-prepared $LiFePO_4$@GNS and it can be seen that all the peaks can be indexed as orthorhombic $LiFePO_4$ (JCPDS No. 40-1499).

Fig. 3a and Fig. S2 (ESI†) show the low-magnification TEM image and scanning electron microscopy (SEM) image, respectively, of the resulting $LiFePO_4$@GNS nanocomposites. Though there are some large particles of ~100 nm in diameter, the majority of the particles were on the scale of tens of nm, indicating that high temperature aggregation or sintering problem was greatly retarded due to the protective graphene shells around each

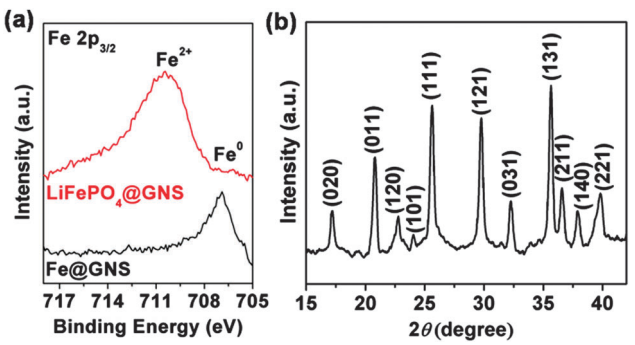

Fig. 2 (a) XPS spectra of Fe $2p_{3/2}$ of $LiFePO_4$@GNS and Fe@GNS. (b) XRD pattern of $LiFePO_4$@GNS.

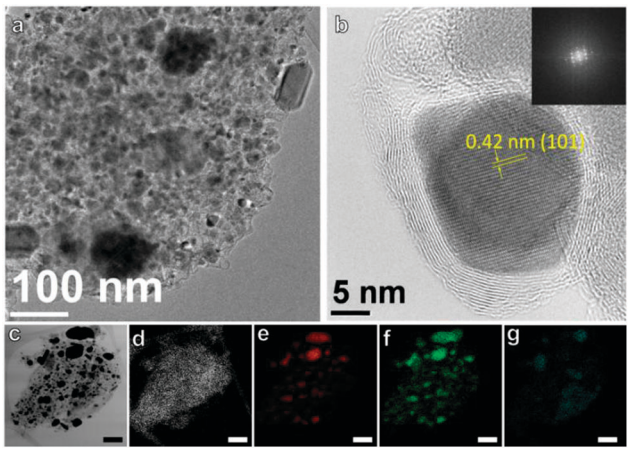

Fig. 3 Characterization of the $LiFePO_4$@GNS nanocomposite. (a) Low magnification TEM image. (b) High magnification TEM image of an individual $LiFePO_4$@GNS nanoparticle, showing the core–shell structure. The inset shows the FFT image of the corresponding nanoparticle, indicating that the nanoparticle is in crystalline form. (c) Energy filter transmission electron microscopy (EFTEM) image of $LiFePO_4$@GNS and corresponding elemental mapping images of (d) carbon, (e) iron, (f) phosphorus and (g) oxygen, showing the similar distributions of these elements. Scale bars in c, d, e, f and g are 100 nm.

individual nanoparticle. The high-magnification TEM image in Fig. 3b reveals the core–shell structure of a typical $LiFePO_4$@GNS nanoparticle (~20 nm in diameter); the core structure of the $LiFePO_4$ was highly crystalline and was coated by uniform and continuous shells consisting of about eight-layer graphene. The contact between the $LiFePO_4$ nanoparticles and surrounding graphene layers ensured effective electron transfer. The carbon content in the composite was estimated to be ~5.1 wt% by the thermogravimetric analysis (TGA) (Fig. S3, ESI†), with the knowledge that the oxidation of $LiFePO_4$ to $Li_3Fe_2(PO_4)_3$ and Fe_2O_3 would result in a weight gain of 5.07 wt%.[15] Elemental mapping analysis in Fig. 3c–g shows similar distributions of C, Fe, P and O. The TEM analysis suggests that the exterior oxygen, lithium and phosphorus sources were able to penetrate through the thin graphene shells to react with the interior iron source to form $LiFePO_4$ without severe aggregation or destroying the graphene shells.

To investigate the electrochemical performance of the $LiFePO_4$@GNS nanocomposite, coin cells were fabricated using metallic lithium foil as the counter electrode, and the working electrode was prepared by mixing the composite with poly(vinylidenedifluoride) (PVDF) at a weight ratio of 90 : 10. Considering the good conductivity of $LiFePO_4$@GNS from the coated graphene shells, no conductive additive was added. Fig. 4a shows the cyclic voltammetry curves at different scan rates. Two redox peaks are observed between 3.3 V and 3.6 V (*vs.* Li/Li^+) at a scan rate of 0.1 mV s^{-1}. These well-defined peaks correspond to the insertion and de-insertion of Li^+ in the $LiFePO_4$ nanoparticles and are still clearly visible at higher scanning rates with wider separation of peak position. Fig. 4b shows the charge–discharge profiles at a current density of 17 mA g^{-1} (corresponding to 0.1 C) and a featured plateau was observed in the charge–discharge curves at a voltage of ~3.45 V that is characteristic of $LiFePO_4$. The small gap (~45 mV) between the charge and discharge plateau indicates that the overpotential during the charge–discharge process was small,

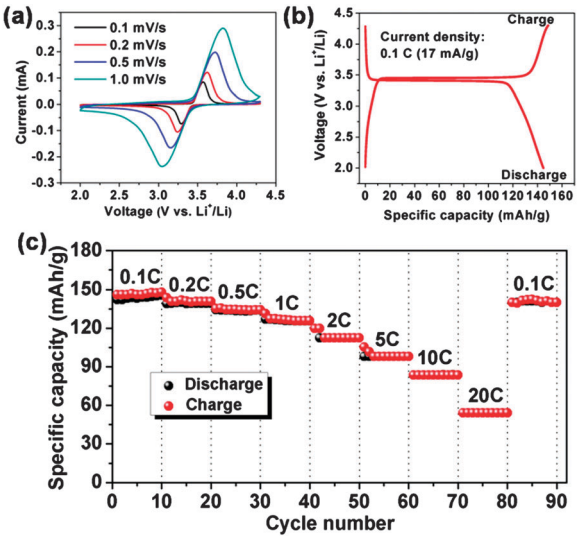

Fig. 4 Electrochemical characterization of the prepared $LiFePO_4$@GNS. (a) Cyclic voltammetry tests at various scan rates in the potential range of 2.0 to 4.3 V (*vs.* Li/Li^+). (b) Charge–discharge profiles at current density of 17 mA g^{-1} (0.1 C) in the potential range of 2.0 to 4.3 V (*vs.* Li/Li^+). (c) The rate performances at different current densities.

which can be ascribed to the good ionic and electronic conductivity of the $LiFePO_4$ nanoparticles coated with conductive graphitic carbon. The discharge and charge specific capacity were calculated to be 145 mA h g^{-1} and 150 mA h g^{-1}, respectively, giving a Coulombic efficiency of 97% for the first cycle at a current density of 17 mA g^{-1}. The relatively low capacity value compared to the theoretical specific capacity (170 mA h g^{-1}) of $LiFePO_4$ may be due to the incomplete crystallization of some of the $LiFePO_4$ nanoparticles, as amorphous nanoparticles encapsulated in graphene shells were observed by careful TEM analysis (Fig. S4, ESI†). The rate capability was evaluated by applying different current densities for the charge–discharge tests and the results are shown in Fig. 4c. At current densities of 170 mA g^{-1} (1 C), 850 mA g^{-1} (5 C) and 1700 mA g^{-1} (10 C), the discharge specific capacities were 128 mA h g^{-1}, 98 mA h g^{-1} and 84 mA h g^{-1}, respectively. At a current density as high as 3400 mA g^{-1} (20 C), the nanocomposite delivered 54 mA h g^{-1}. When the current density was cycled back to 17 mA g^{-1}, the discharge specific capacity remained at 143 mA h g^{-1}, demonstrating its high power performance and stability.

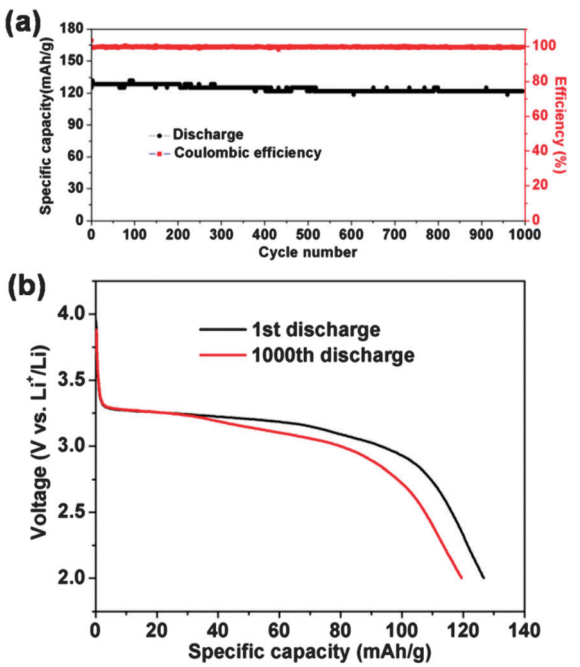

Fig. 5 (a) Cycling performances at current density of 170 mA g^{-1} (1 C) between 2.0 and 4.3 V. (b) Discharge profiles for the 1st and 1000th cycles.

To examine the long-term cycle performance of the as-prepared $LiFePO_4$@GNS electrode, it was cycled at a current density of 170 mA g^{-1} and after 1000 cycles, the specific capacity remained at 122 mA h g^{-1} with 95.3% retention compared with that of the first cycle as shown in Fig. 5a. In addition, the discharge curves (Fig. 5b) of 1st cycle and 1000th cycle retained a similar shape, suggesting its excellent cycle performance.

In summary, highly crystalline $LiFePO_4$ nanoparticles encapsulated in continuous and uniform graphene nanoshells have been synthesized by solid state reaction between carbon-coated Fe nanoparticles and LiH_2PO_4. When used as a lithium ion battery cathode, the $LiFePO_4$@GNS exhibits excellent cycling stability and rate capability, which can be ascribed to the fast ionic diffusion in the crystalline nano-sized $LiFePO_4$ as well as the efficient electron transport and transfer that benefits from the highly conductive graphitic carbon coatings. The current process could be extended to the preparation of other carbon-coated lithium metal oxide nanocomposites for use in lithium ion battery materials.

The Office of Naval Research MURI program (#00006766, N00014-09-1066), Air Force Office of Scientific Research MURI (FA9550-12-1-0035) and Air Force Office of Scientific Research (FA9550-09-1-0581) funded this research.

Notes and references

1 Y. Wang, Y. Wang, E. Hosono, K. Wang and H. Zhou, *Angew. Chem., Int. Ed.*, 2008, **47**, 7461.
2 L. Shen, H. Li, E. Uchaker, X. Zhang and G. Cao, *Nano Lett.*, 2012, **12**, 5673.
3 B. Kang and G. Ceder, *Nature*, 2009, **458**, 190.
4 P. S. Herle, B. Ellis, N. Coombs and L. F. Nazar, *Nat. Mater.*, 2004, **3**, 147.
5 Z. Chen, Y. Qin, K. Amine and Y. K. Sun, *J. Mater. Chem.*, 2010, **20**, 7606.
6 M. M. Doeff, J. D. Wilcox, R. Kostecki and G. Lau, *J. Power Sources*, 2006, **163**, 180.
7 J. Wang and X. Sun, *Energy Environ. Sci.*, 2012, **5**, 5163.
8 K. Dokko, K. Shiraishi and K. Kanamura, *J. Electrochem. Soc.*, 2005, **152**, A2199.
9 H. Li and H. Zhou, *Chem. Commun.*, 2012, **48**, 1201.
10 J. Yang, J. Wang, Y. Tang, D. Wang, X. Li, Y. Hu, R. Li, G. Liang, T. K. Sham and X. Sun, *Energy Environ. Sci.*, 2013, **6**, 1521.
11 J. D. Wilcox, M. M. Doeff, M. Marcinek and R. Kostecki, *J. Electrochem. Soc.*, 2007, **154**, A389.
12 Y. D. Cho, G. T. K. Fey and H. M. Kao, *J. Power Sources*, 2009, **189**, 256.
13 H. Fei, Z. Peng, L. Li, Y. Yang, W. Lu, E. L. G. Samuel, X. Fan and J. M. Tour, *Nano Res.*, 2014, **7**, 502–510.
14 T. Fujii, F. M. F. de Groot, G. A. Sawatzky, F. C. Voogt, T. Hibma and K. Okada, *Phys. Rev. B*, 1999, **59**, 3195.
15 J. Yang, J. Wang, X. Li, D. Wang, J. Liu, G. Liang, M. Gauthier, Y. Li, D. Geng, R. Li and X. Sun, *J. Mater. Chem.*, 2012, **22**, 7537.